



Sudden Unexpected Death in Epilepsy and Respiratory Defects in a Mouse Model of DEPDC5-Related Epilepsy

Hsin-Yi Kao, PhD,¹ Yilong Yao, PhD,² Tao Yang, PhD,¹ Julie Ziobro, MD, PhD,³ Mary Zylinski, BS,² Mohd Yaqub Mir, PhD,² Shuntong Hu, MD, PhD ,¹ Runnan Cao, PhD,⁴ Nurun Nahar Borna, MD, PhD,¹ Rajat Banerjee, PhD,¹ Jack M. Parent, MD,^{1,5,6} Shuo Wang, PhD,⁴ Daniel K. Leventhal,^{1,5,7,8} Peng Li, PhD,^{2,6,9,10} and Yu Wang, MD, PhD ^{1,5,6}

Objectives: *DEPDC5* is a common causative gene in familial focal epilepsy with or without malformations of cortical development. Its pathogenic variants also confer a significantly higher risk for sudden unexpected death in epilepsy (SUDEP), providing opportunities to investigate the pathophysiology intersecting neurodevelopment, epilepsy, and cardiorespiratory function. There is an urgent need to gain a mechanistic understanding of DEPDC5-related epilepsy and SUDEP, identify biomarkers for patients at high risk, and develop preventive interventions.

Methods: *Depdc5* was specifically deleted in excitatory or inhibitory neurons in the mouse brain to determine neuronal subtypes that drive epileptogenesis and SUDEP. Electroencephalogram (EEG), cardiac, and respiratory recordings were performed to determine cardiorespiratory phenotypes associated with SUDEP. Baseline respiratory function and the response to hypoxia challenge were also studied in these mice.

Results: *Depdc5* deletion in excitatory neurons in cortical layer 5 and dentate gyrus caused frequent generalized tonic-clonic seizures and SUDEP in young adult mice, but *Depdc5* deletion in cortical interneurons did not. EEG suppression immediately following ictal offset was observed in fatal and non-fatal seizures, but low amplitude rhythmic theta frequency activity was lost only in fatal seizures. In addition, these mice developed baseline respiratory dysfunction prior to SUDEP, during which ictal apnea occurred long before terminal cardiac asystole.

Interpretation: *Depdc5* deletion in excitatory neurons is sufficient to cause DEPDC5-related epilepsy and SUDEP. Ictal apnea and respiratory dysregulation play critical roles in SUDEP. Our study also provides a novel mouse model to investigate the underlying mechanisms of DEPDC5-related epilepsy and SUDEP.

ANN NEUROL 2023;00:1–13

Epilepsy affects more than 70 million people globally. Sudden unexpected death in epilepsy (SUDEP) has a global incidence of 0.22 to 1.2 of 1,000 individuals/year,¹ accounting for up to 17% of death in patients with epilepsy, second only to stroke in potential life-years lost due

to neurological diseases.² The etiology of SUDEP is heterogeneous, including cardiac, respiratory, and autonomic dysregulation in different epilepsy syndromes.² Previous SUDEP studies focused primarily on channelopathies. For example, *SCN1A* encodes the alpha-subunit of the

View this article online at [wileyonlinelibrary.com](https://onlinelibrary.wiley.com/doi/10.1002/ana.26773). DOI: 10.1002/ana.26773

Received Jan 19, 2023, and in revised form Aug 7, 2023. Accepted for publication Aug 9, 2023.

Address correspondence to Dr Yu Wang, Department of Neurology, University of Michigan, Ann Arbor, MI, USA. E-mail: eegwang@med.umich.edu and Dr Peng Li, VA Ann Arbor Healthcare System, Ann Arbor, MI 48105, USA. E-mail: penglium@umich.edu

Hsin-Yi Kao, Yilong Yao these authors contributed equally to this work.

From the ¹Department of Neurology, University of Michigan, Ann Arbor, MI; ²Life Sciences Institute, University of Michigan, Ann Arbor, MI; ³Department of Pediatrics, University of Michigan, Ann Arbor, MI; ⁴Department of Radiology, Washington University in St. Louis, St. Louis, MO; ⁵VA Ann Arbor Healthcare System, Ann Arbor, MI; ⁶Michigan Neuroscience Institute, University of Michigan, Ann Arbor, MI; ⁷Department of Biomedical Engineering, University of Michigan, Ann Arbor, MI; ⁸Parkinson Disease Foundation Research Center of Excellence, University of Michigan, Ann Arbor, MI; ⁹Department of Biologic and Material Sciences, University of Michigan, Ann Arbor, MI; and ¹⁰Department of Molecular and Integrative Physiology, University of Michigan, Ann Arbor, MI

voltage-gated sodium channel Nav1.1 in the mammalian brain and heart. Its pathogenic variants were identified in > 70% of children with Dravet syndrome whose SUDEP risk was estimated to be 15-fold greater than other childhood-onset epilepsies.³ Other channelopathies also affect the brain and heart, suggesting that they could confer a higher risk of SUDEP via direct effects on cardiac functions. Therefore, a “brain-heart” hypothesis for SUDEP has been proposed.⁴ On the other hand, Kim et al concluded that SUDEP in patients with Dravet syndrome resulted from primary central apnea.⁵ This hypothesis was supported in *Scn8a* mutant mice that developed apnea during the tonic phase of a seizure and failed to resume breathing.⁶

Pathogenic variants of *DEPDC5*, an important gene in the mTOR signaling pathway, were first identified in 7 large families with familial focal epilepsy with variable foci and in approximately 12% of smaller families with focal epilepsy.⁷ The Epi4K consortium and Epilepsy Phenome/Genome Project collaborations later demonstrated that among the top 5 most enriched genes for epilepsy risk, only *DEPDC5* reached the study-wide significant enrichment for familial non-acquired focal epilepsy.⁸ Meanwhile, several studies suggested that pathogenic variants of *DEPDC5* significantly increase the risk of SUDEP.^{9–12} For example, *DEPDC5* variants were found in approximately 10% of cases in a retrospective SUDEP cohort.¹⁰ In contrast to channelopathies, *DEPDC5*-related epilepsy primarily manifests as a focal lesion in the brain.^{13,14} Whereas patients with tuberous sclerosis complex (TSC), the prototypical monogenic disorder of the mTOR pathway, develop widespread developmental lesions in the brain and other organ systems (eg, skin, heart, and kidneys),¹⁵ patients with *DEPDC5*-related epilepsy have no extra-neural lesions.^{13,14} For example, 16 patients with GTPase-activating protein activity toward Rags-1 (GATOR1)-related epilepsy showed no evidence of cardiac arrhythmia or structural abnormality on Holter monitoring and transthoracic echocardiogram. More importantly, no clinical cardiac anomalies were detected in 3 of 3 patients carrying pathogenic *DEPDC5* pathogenic variants who succumbed to SUDEP.⁹

Understanding the pathophysiology of *DEPDC5*-related SUDEP has significant clinical implications. Such knowledge could identify preventable causes and biomarkers for patients at high risk of SUDEP. However, the lack of an animal model that reliably and faithfully recapitulates the human phenotype has made it challenging to parse out the mechanisms. For example, mice with *Emx1*-Cre mediated conditional knockout of *Depdc5* in dorsal cortical progenitors that give rise to excitatory neurons and astrocytes died around postnatal day (P)16 to 18. These mice developed clusters of tonic-clonic seizures, status epilepticus, wasting,

and malnutrition, making it difficult to determine the cause of death.^{16,17} On the other hand, mice with a pan-neuronal knockout of *Depdc5* died after a single terminal seizure at 3 months of age.^{9,18} Interestingly, the majority of these mice had no history of seizures, representing an extremely rare patient event. In this study, we showed that *Depdc5* deletion in a subpopulation of mouse forebrain excitatory neurons caused frequent generalized tonic-clonic seizures in young adult mice. These mice eventually developed SUDEP. The respiratory recording showed interictal respiratory dysregulation and ictal apnea long before the terminal cardiac asystole. Our studies provide a refined framework to further investigate the pathophysiology of *DEPDC5*-related epilepsy and SUDEP at molecular, cellular, and circuit levels.

Materials and Methods

Animals

Rbp4-Cre transgenic mice (B6.FVB(Cg)-Tg (Rbp4-Cre) KL100Gsat/Mmucd, RRID: MMRRC_037128-UCD, donated by Dr. Kenneth Kwon at the University of Michigan) were crossed with mice with floxed alleles of *Depdc5*^{F/F} (*Depdc5*^{tm1c} (EUCOMM)Hmgu, donated by Dr. Jun Hee Lee at the University of Michigan) to generate *Depdc5* conditional knockout (CKO) mice. Ventral medial ganglionic eminence (MGE) progenitor-specific Nkx2.1-Cre transgenic mice (Jackson Laboratories #008661) were used to generate interneuron-specific *Depdc5* CKO mice. Ai9 mice (B6.Cg-Gt(ROSA)26Sor^{tm9(CAG-tdTomato)Hze}/J, Jackson Laboratories #007909) were used to label cells with recombinase activity mediated by Rbp4-Cre. Male homozygous floxed *Depdc5* mice (*Depdc5*^{F/F}) were bred with female mice heterozygous for floxed *Depdc5* (*Depdc5*^{F/W}) and heterozygous for the Cre allele to generate litters of homozygous CKO (Rbp4-Cre; *Depdc5*^{F/F} or Nkx2.1-Cre; *Depdc5*^{F/F}), heterozygous CKO (Rbp4-Cre; *Depdc5*^{F/W} or Nkx2.1-Cre; *Depdc5*^{F/W}), and wild-type (WT) (*Depdc5*^{F/F} or *Depdc5*^{F/W}) mice. Because our pilot study showed that Rbp4-Cre; *Depdc5*^{F/W} displayed no pathological or epileptic phenotypes, in addition to previous studies showing that *Emx1*-Cre; *Depdc5*^{F/W} and *Syn1*-Cre; *Depdc5*^{F/W} had no phenotypes,^{16–18} Rbp4-Cre; *Depdc5*^{F/W} mice were also used as littermate controls. DNA was extracted from mouse tail biopsies using the Extract-N-Amp Tissue polymerase chain reaction (PCR) kit (Sigma; XNAT2-1KT) according to the manufacturer's instructions. Genotyping of the *Depdc5* gene was performed using primers (forward: 5'-CTGGAATACAGGGGGTAAGCCAGTG-3'; and reverse: 5'-CAGGACTACACAGAGAAACCCTGTCTC-3') that flank LoxP sites surrounding exon 5, allowing concurrent detection of the WT and conditional alleles. Agarose gel electrophoresis was performed to detect a 177-base pair (bp) band for the WT allele and a 337-bp band for LoxP conditional allele. The presence of the Rbp4-Cre recombinase gene was determined using primers (forward: 5'-GGGCGCCTCGTCCCTC-3'; and reverse: 5'-CCCCAGAAATGCCAGATTACGTAT-3') to detect a 600 bp band. The presence of the Nkx2.1-Cre recombinase gene was determined

using primers (forward: 5'-CTCTGGTGGCTGCCTAAAAC-3'; and reverse: 5'-CGGTTATTCAACTTGCACCA-3') detecting a 410 bp band. All mice were housed in a 12-hour light–dark cycle, climate-controlled room, with access to food and water ad libitum. The protocol for the study has received approval from the Institutional Animal Care and Use Committee at the University of Michigan, and all studies were conducted in accordance with the United States Public Health Service's Policy on Humane Care and Use of Laboratory Animals.

Immunohistochemistry

Brains were removed and fixed in 4% paraformaldehyde in phosphate-buffered saline after transcardial perfusion, sectioned at 50 μ m on a Leica VT1000S vibratome, and processed for immunocytochemistry as free-floating sections. Primary antibodies included rabbit anti-Parvalbumin (1:1000; Abcam; Cat# ab181086), rabbit anti-GFAP (1:1000; Abcam; Cat# ab7260), and rabbit anti-phospho-S6 ribosomal protein Ser 235/236 (1:2000; Cell Signaling). Fluorescently conjugated secondary antibodies (Alexa Fluor 488, 594, or 647, 1:500) were obtained from Molecular Probes, and nuclei were labeled with bisbenzimidazole (Molecular Probes; Cat# H1398).

Electroencephalogram (EEG) Implantation and Analysis

To determine if Rbp4-Cre; *Depdc5*^{F/F} and Nkx2.1-Cre; *Depdc5*^{F/F} CKO mice exhibit electroclinical seizures and interictal epileptiform discharges (IEDs), we monitored animals with continuous video-electroencephalogram (vEEG; Natus, Middleton, WI). Mice were implanted with three epidural screw electrodes (E363/96; P1 Technologies, Roanoke, VA) at P30. Procedures for affixing electrodes were performed as previously described.¹⁶ Three electrodes were positioned and fastened through burr holes, with 2 electrodes implanted over the left and right parietal lobes and a reference electrode implanted over the cerebellum. The sockets were fitted into a 6-pin electrode pedestal, and the entire apparatus was secured with dental cement (Stoelting). Five days after surgery, the animals were monitored continuously for up to 60 days or until death. Recordings were sampled at 4096 Hz and analyzed offline with concurrent video. Seizures and epileptiform activity were assessed manually in their entirety by fellowship-trained and board-certified epileptologists blinded to the genotype. IEDs were defined as transients distinguishable from background activity with characteristic morphology typically, but neither exclusively nor invariably, found in interictal EEGs of people with epilepsy¹⁹ and had to meet at least 3 of following criteria: (1) di- or tri-phasic waves with a sharp wave or spike morphology (< 200 msec duration); (2) different waveform from the ongoing background activity; (3) asymmetry of the waveform: a sharply ascending phase and a slower descending phase, or vice versa; (4) the transient is followed by an associated after-going slow wave; and (5) the background activity is disrupted by the presence of the epileptiform discharges. Seizures were defined as EEG phenomena consisting of repetitive epileptiform discharges at > 2 cycles/second and/or a characteristic pattern with quasi-rhythmic spatiotemporal evolution (ie, gradual change in frequency, amplitude, morphology, and

location) lasting at least several seconds (usually > 10 seconds). Two other short-duration (< 10 seconds) EEG seizure patterns were defined as electro-decrement or low voltage fast activity seen during clinically apparent epileptic seizures. EEG seizure patterns unaccompanied by behavioral epileptic manifestations were referred to as electrographic or subclinical seizures.¹⁹ Mice with dislodged EEG head caps were excluded from the study.

Recordings in European Data Format (EDF) were transformed using the “edfread” function in MATLAB. Spectrograms were constructed using the MATLAB “fft” function to analyze data from 10 minutes before to 10 minutes after seizure offset in rectangular 1-second windows without overlap. Signal power at 1 to 70 Hz was represented in the spectrograms on a log scale. Differences in the time-frequency spectrograms between fatal and non-fatal seizures were evaluated with a shuffle test. For the 24 seizures reported (16 non-fatal and 8 fatal), the difference between the mean non-fatal and mean fatal spectrograms were calculated for 600 seconds preceding and following seizure offset. To generate a surrogate distribution of differences in the mean spectrograms, the labels “fatal” and “non-fatal” were randomly assigned to each seizure, and the difference in mean spectrograms was recalculated. This was repeated 10,000 times. The *p* value testing the null hypothesis of no difference between fatal and non-fatal seizures at each time-frequency point was determined as the fraction of surrogate differences greater than the true difference. The *p* values were smoothed using a 2D Gaussian filter with a standard deviation of 0.5.

Simultaneous Recording of EEG, Electrocardiogram, and Breathing During SUDEP

Mice around 2 months old were implanted with EEG and electrocardiogram (ECG) electrodes. For EEG electrodes, 2 holes were drilled into the skull (one on the parietal bone and the other above the cerebellum), and electrodes were positioned and fastened using mounting screws (E363/96). For ECG electrodes, the wires were bilaterally connected to the tissue under the skin on the side of the body and extended subcutaneously to the head. Both EEG and ECG electrodes were connected to the head mount, which was stabilized by dental cement. After 1 week of recovery, mice were placed in the whole-body plethysmograph chamber (Buxco; approximately 500 mL), and the head mount was connected to the amplifier. EEG, ECG, and breathing data were collected by PowerLab (AD instruments). The sampling rate was 1,000 Hz. The EEG signal was digitally filtered using a band-pass filter (25–300 Hz) and integrated (time constant of 0.1 seconds) by LabChart (AD instruments). The ECG signal was digitally filtered using a high-pass filter (25 Hz). The mice were recorded daily until they developed SUDEP.

Breathing Recording in Hypoxia Challenge

For breathing recording in the basal and hypoxia condition, mice were placed in the whole-body plethysmography chamber at room temperature. Mice were allowed to acclimate to the chamber in normoxia (21% O₂ balanced with nitrogen) at 1 L/minute flow rate before recording breathing. For the hypoxia challenge, mice were exposed to normoxia for 20 minutes and then switched to hypoxia (10% O₂ balanced by nitrogen) for

20 minutes before switching back to normoxia. During the switches, the chamber was flushed with the new gas mixture for 1 minute before data collection. Breathing parameters were recorded and analyzed by EMKA IOX2 software (EMKA Technologies, Beijing, China) that calculates the tidal volume based on the Drorbaugh and Fenn formula.²⁰ Body temperature was tested by a rectal probe connected to a temperature controller (Physitemp Instruments; TCAT-2LV) in the hypoxia challenge.

Image Acquisition, Soma Size, Cortical Thickness Measurement, and Statistical Analyses

Multi-channel imaging was performed using a Leica SP5 confocal microscope. All images were further processed in Adobe Photoshop software. The soma size of Ai9+ or PV+ neurons from approximately P21 to 30 brains were compared between control and *Depdc5* CKO. Cortical thickness was measured from the pial surface to the white matter from the somatosensory cortex. Automated measurement was performed in ImageJ. Statistical analysis was performed using GraphPad. The number of animals used in each experiment was listed in the results and figure legends. The *p* values were determined by the Student *t* test. Analysis of variance was conducted with Bonferroni post hoc correction for multiple comparisons. All data were shown as mean \pm SEM. A *p* value less than 0.05 was considered to be statistically significant. In figure panels throughout the paper, the following labeling conventions for statistical testing are used: no significance (ns): $p > 0.05$; * $p < 0.05$; ** $p < 0.01$; *** $p < 0.001$; and **** $p < 0.0001$.

Results

Depdc5 Deletion in a Subpopulation of Forebrain Excitatory Neurons Causes Epilepsy

We and others have shown that *Emx1*-Cre mediated *Depdc5* deletion in dorsal cortical progenitors causes severe epilepsy, megalencephaly, and premature death around postnatal (P) weeks 2 to 3.^{16,17} Surprisingly, *Syn1*-Cre mediated *Depdc5* deletion in all neuronal lineages (excitatory and inhibitory neurons) and neural structures often caused just one terminal seizure followed by death at 3 months old.^{9,18} These striking phenotypic differences suggest that epileptogenesis and SUDEP in *DEPDC5*-related epilepsy could be cell-type dependent.

To test whether *Depdc5* deletion in excitatory neurons alone causes epilepsy, we crossed *Rbp4*-Cre transgenic mice²¹ to mice with floxed *Depdc5* alleles¹⁶ to delete *Depdc5* in a subset of forebrain excitatory neurons as early as at embryonic day (E) 16.5²¹ (hereafter referred to as *Rbp4*-Cre; *Depdc5*^{F/F} CKO mice). To examine the recombination pattern, we first crossed *Rbp4*-Cre to the Ai9 reporter line.²² tdTomato signal was observed in the somata, dendrites, and axons of layer 5 pyramidal and dentate gyrus granule excitatory neurons (Fig 1A), consistent with the previous report.²¹ Furthermore, these tdTomato labeled cells were not immunopositive for markers of interneurons (Fig 1B), astrocytes (Fig 1C), or

oligodendrocytes (data not shown), suggesting that *Rbp4*-Cre recombinase activity is both spatially and cell-type specific. We then crossed *Rbp4*-Cre to both Ai9 and *Depdc5*^{F/F} transgenic lines to generate *Depdc5* conditional knockout (*Rbp4*-Cre; Ai9; and *Depdc5*^{F/F}) and littermate controls (*Rbp4*-Cre; Ai9; *Depdc5*^{F/W} or *Rbp4*-Cre; Ai9; *Depdc5*^{W/W}). Because of the lack of a specific antibody against *DEPDC5*, immunohistochemistry and Western blot could not be performed to directly detect the Cre-mediated *Depdc5* deletion. Instead, we examined the expression level of ribosomal protein S6 (pS6), the downstream target of the mTOR signaling pathway. Compared to layer 4 or 6 neurons (tdTomato negative), layer 5 *Depdc5* knock-out (KO) neurons (tdTomato positive) in the same *Rbp4*-Cre; *Depdc5*^{F/F} CKO mice brain showed a robust increase in pS6 immunoreactivity (Fig 1D, D'), indicating elevated mTOR signaling. Compared to layer 5 WT neurons, layer 5 *Depdc5* KO neurons also showed significantly increased pS6 staining (data not shown) with a much larger soma surface area (Fig 1E–G), a pathological hallmark of mTORopathies. Cortical thickness, however, was not significantly increased in *Rbp4*-Cre; *Depdc5*^{F/F} CKO mice (Fig 1H).

To determine whether *Depdc5* deletion mediated by *Rbp4*-Cre is sufficient to cause spontaneous seizures, continuous vEEG monitoring was performed (Fig 2A, n = 19). All *Rbp4*-Cre; *Depdc5*^{F/F} CKO mice developed IEDs, including spike and wave discharges that at times were periodic or rhythmic and lasted up to several seconds (Fig 2B, B'). Mice developed their first seizures by 2 months old (postnatal day 57.25 \pm 10.92 days old). The seizure frequency was 1.49 \pm 0.83 per day (Fig 2D, F). Most seizures were characterized by generalized tonic-clonic (GTC) activity followed by wild running (Racine score 5, n = 122 out of 126),²³ and a few were subclinical seizures (n = 4 out of 126). All seizures showed bi-hemispheric onset with rhythmic spike-and-wave discharges followed by evolution in frequency and amplitude (Fig 2C, C'). Seizures were brief (Fig 2E), and no animals developed status epilepticus (defined as lasting longer than 3 minutes) or seizure clusters (defined as > 2 seizures within 1 hour). In contrast, *Rbp4*-Cre; *Depdc5*^{F/W} mice (n = 11) did not show IED or spontaneous seizures.

To test if *Depdc5* deletion in interneurons (IN) causes epilepsy, we deleted *Depdc5* in ventral cortical progenitors within the MGE using *Nkx2.1*-Cre transgenic mice.²⁴ The MGE is the primary source of parvalbumin (PV) and somatostatin (SST) interneurons²⁵ that respectively provide the major contribution to perisomatic and dendritic inhibition.²⁶ Cre expression in *Nkx2.1*-Cre mice was detected in the MGE as early as E10.5 and postnatally in more than 80% of PV- and SST-positive INs.²⁴

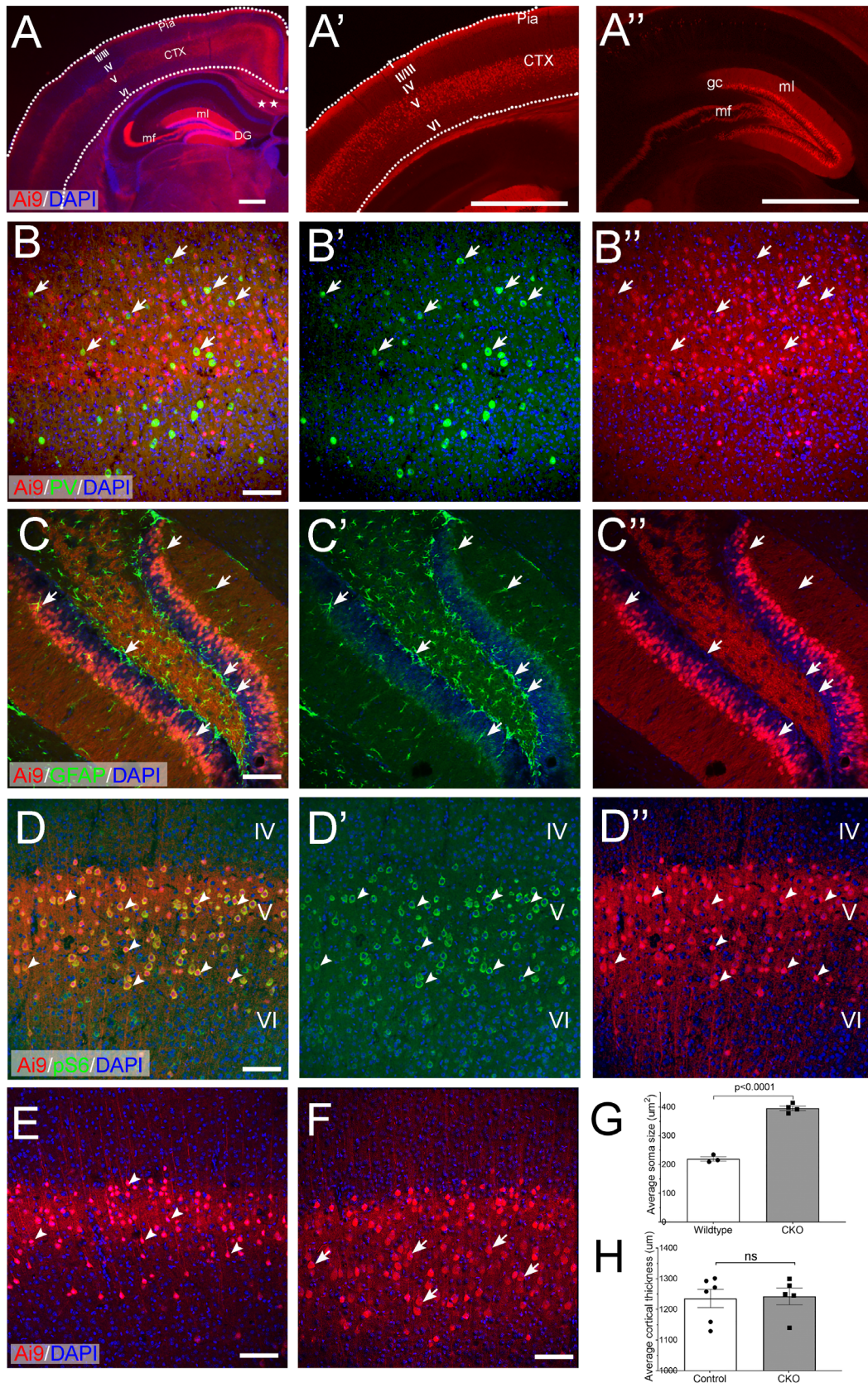


(Figure legend continues on next page.)

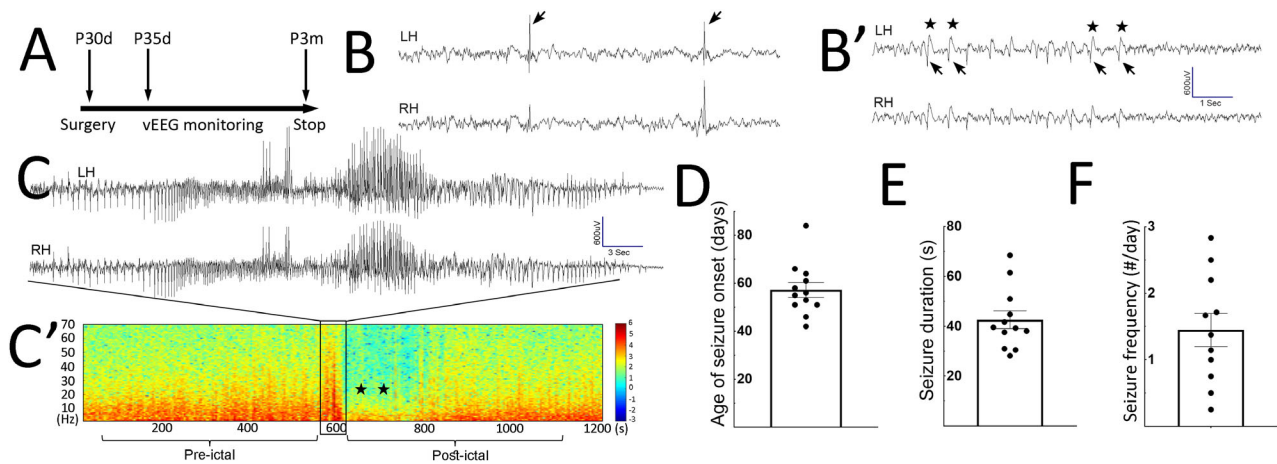


FIGURE 2: *Rbp4-Cre; Depdc5^{F/F}* CKO mice develop spontaneous generalized tonic-clonic seizures. (A) Timeline of continuous vEEG monitoring experiments. The EEG implantation was performed around one-month-old. The vEEG started 5 days after implantation and continued until P3 months (m). (B, B') Representative examples of interictal epileptiform discharges (IEDs), including singly occurred spikes in (B) and periodic spike-and-wave discharges in (B'). In (B'), arrows indicate spikes, and stars indicate the after-going slow waves. (C) A representative EEG trace of generalized tonic-clonic seizures. (C') The spectrogram of the seizure in (C). The boxed area displays a surge of increased power across all frequency bands, representing the seizure in (C). Postictally, decreased power in all frequency bands (stars) is evident and represents EEG background suppression, lasting up to 200 seconds (s). The background then gradually recovers. (D-F) Age of seizure onset = 57.25 ± 3.16 postnatal days ($n = 12$), seizure duration (42.65 ± 3.544 seconds, $n = 12$), and seizure frequency (1.45 ± 0.25 per day, $n = 11$). LH = left hemisphere; RH = right hemisphere.

Although PV+ INs were cytomegalic with significantly increased pS6 immunostaining (Fig 3A–C), *Nkx2.1-Cre; Depdc5^{F/F}* CKO mice showed no change in cortical thickness (Fig 3D) and no seizures during 2 to 6 weeks of continuous vEEG recording (data not shown). In summary, our data suggest that *Depdc5* deletion in a subpopulation of excitatory neurons in the brain is sufficient to drive epileptogenesis and cause seizures.

***Rbp4-Cre; Depdc5^{F/F}* CKO Mice Develop SUDEP**

Rbp4-Cre; Depdc5^{F/F} CKO mice grew normally into young adulthood but had a shortened life span (Fig 4A). Nearly all *Rbp4-Cre; Depdc5^{F/F}* CKO mice died suddenly without physical or behavioral concerns. The carcasses were often in a tonic posture with extended hindlimbs, raising concern for SUDEP. Littermate WT and

Rbp4-Cre; Depdc5^{F/W} mice all survived beyond 6 months. Continuous vEEG monitoring was performed to identify SUDEP. Eight of 12 *Rbp4-Cre; Depdc5^{F/F}* CKO mice died immediately following a generalized tonic-clonic seizure (Racine score of 5). The fatal and the last non-fatal seizures from the same animal were analyzed to investigate if EEG features could predict SUDEP. The EEG signals started recovering within 10 to 30 seconds from the onset of post-ictal suppression in non-fatal seizures, whereas the EEG signals never recovered from the suppression in fatal seizures (Fig 4B, C). Visual inspection of the post-ictal EEG revealed that all non-fatal seizures preserved low amplitude rhythmic theta frequency activity, whereas fatal seizures did not (see Fig 4B, C inserts), which was confirmed by a statistically significant difference in theta power immediately after seizures (see Fig 4D, D'). The

FIGURE 1: *Rbp4-Cre* mediates *Depdc5* deletion in cortical layer V and dentate gyrus excitatory neurons. (A) A representative coronal section of an *Rbp4-Cre; Ai9* mouse brain. In the cortex, tdTomato-positive neurons are in cortical layer V and send out interhemispheric cortical-to-cortical axonal projection (stars). In the hippocampus, granular cells (gc) in the dentate gyrus (DG), mossy fibers (mfs), and dendrites in the molecular layer (ml) are intensely labeled. (A' and A'') Are higher magnification images of the cortex and hippocampus, respectively. Dotted lines are drawn to outline the cortex. Roman numerals indicate different cortical layers. CTX: cortex. (B–B'') tdTomato-positive cells are not positive for the interneuron marker, Parvalbumin (green arrows), or C-C'' the astrocyte marker, GFAP (green arrows). (D–D'') Representative images obtained from an *Rbp4-Cre; Depdc5^{F/F}; Ai9^{+/-}* mouse brain. In the cortex, dtTomato-positive *Depdc5* knockout (KO) neurons in layer V have significantly increased immunoreactivity of pS6 (green), as compared to dtTomato-negative neurons in layers IV and VI. (E–G) Compared to dtTomato-positive layer V neurons in control animals (E; arrowheads), dtTomato-positive *Depdc5* KO neurons (F; arrows) are cytomegalic and have a significantly increased surface area (G; control: $219.7 \pm 7.46 \mu\text{m}^2$, $n = 3$, vs conditional knockout [CKO] $395.5 \pm 7.64 \mu\text{m}^2$, $n = 4$, $p < 0.0001$). (H) Cortical thickness is not increased in *Rbp4-Cre; Depdc5* CKO mice (control: $1235 \pm 49.97 \mu\text{m}$, $n = 6$ vs CKO $1262 \pm 34.9 \mu\text{m}$, $n = 5$, $p = 0.6$). Scale bar = 250 μm in A; 1 mm in A' and A''; 100 μm in B to F.

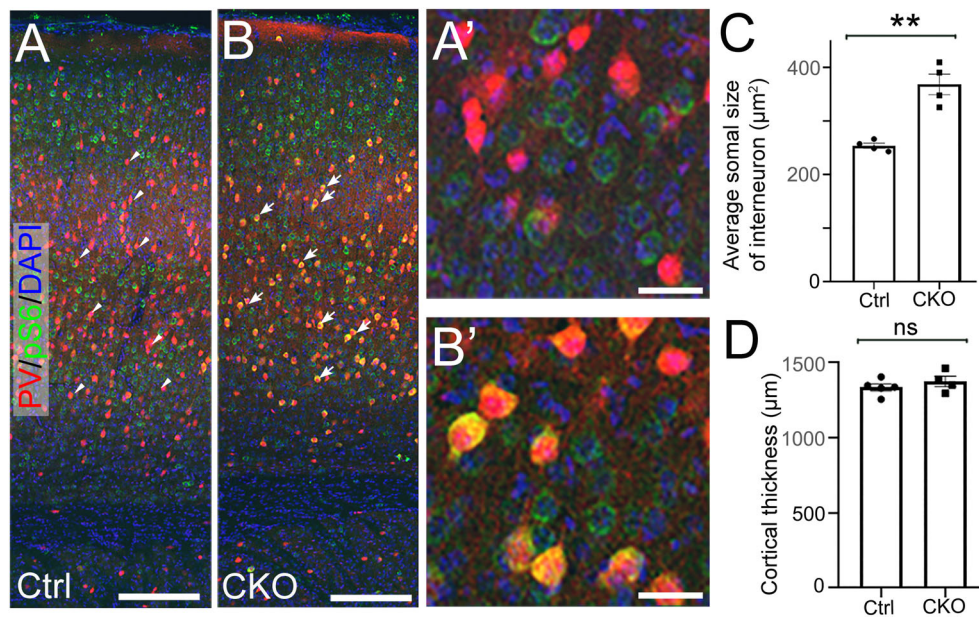


FIGURE 3: *Depdc5* deletion in interneurons does not cause seizures. (A, B) Representative images of anti-pS6 (green) and anti-PV (red) co-immunohistochemistry staining on P21 brain coronal sections from control (A) and *Nkx2.1-Cre; Depdc5* CKO mice. Compared to control PV+ interneurons (arrowheads in A), *Depdc5* KO PV+ interneurons (arrows in B) show significantly increased immunoreactivity of pS6 (yellow). (A' and B') Are higher magnification images. (C) Quantification shows that cortical PV + interneurons in *Nkx2.1-Cre; Depdc5^{F/F}* CKO mice have an enlarged soma size ($n = 4$ in control and CKO groups, student *t* test, $p < 0.001$). (D) *Nkx2.1-Cre; Depdc5* CKO mice do not display increased cortical thickness. Scale bars = 500 μm in A and B; and 25 μm in A' and B'. CKO = conditional knockout; Ctrl = control; ns = not significant; PV+ = parvalbumin positive.

absence of this specific theta frequency (3–12 Hz) band could suggest that “death” already occurred before the seizure offset or could represent a unique electrographic marker indicating imminent death or an irreversible pathological state. Because the seizure was brief and cardiac asystole did not occur ictally (see the next section), the immediate EEG suppression likely represented an abrupt and widespread circuit perturbation that is not reversible and results in death. Semiologically, there was no difference in severity between the fatal and last non-fatal seizure because most seizures in each group were GTC (Fig 4E). The seizure duration did not differ between the fatal and last non-fatal seizure (Fig 4F). The frequency of non-fatal seizures did not increase before the terminal seizure (Fig 4G). Fatal seizures occurred during both the nocturnal and diurnal phases (4 in the light phase and 4 in the dark phase). The age at SUDEP ranged from P46 to 116 days (Fig 4H). Our data show that the *Rbp4-Cre; Depdc5^{F/F}* CKO mouse model recapitulates many features of epilepsy and SUDEP in humans.

***Rbp4-Cre; Depdc5^{F/F}* CKO Mice Develop Ictal Apnea and Interictal Respiratory Dysregulation**

To better understand the cause of post-ictal death in *Rbp4-Cre; Depdc5^{F/F}* CKO mice, a custom mouse

epilepsy monitoring unit was used to record EEG, ECG, behavior, and plethysmography. Mice were singly housed in a plethysmography recording chamber and underwent daily 12-hour recording sessions until they developed SUDEP. Although the majority of SUDEP events occurred when the recording was temporarily halted or after the recording apparatus was dislodged, 3 SUDEP events were recorded and analyzed. Pre-ictally, *Rbp4-Cre; Depdc5^{F/F}* CKO mice exhibited rhythmic breathing and heartbeats (Fig 5A, B, B1 enlarged from B). Interestingly, slightly before ictal onset detected by EEG (Fig 5C1, arrow), *Rbp4-Cre; Depdc5^{F/F}* CKO mice already increased their breathing rate (see Fig 5C1, arrowhead) without clear body movements detected on video or by movement artifacts on EEG. During fatal seizures, tachypnea continued into the ictal period and then abruptly developed into complete apnea (Fig 5D1, red arrowhead), which persisted into the post-ictal period and never recovered (Fig 5E). Modest bradycardia was seen during the post-ictal phase, but the heartbeat continued for several minutes with slowly worsening bradycardia, eventually leading to terminal asystole (see Fig 5E1 enlarged from E). It is noteworthy that the clinical and electrographic seizure was still ongoing after the onset of apnea. In contrast, tachypnea was observed through the ictal and post-ictal periods during non-fatal seizures. These results suggest the critical role

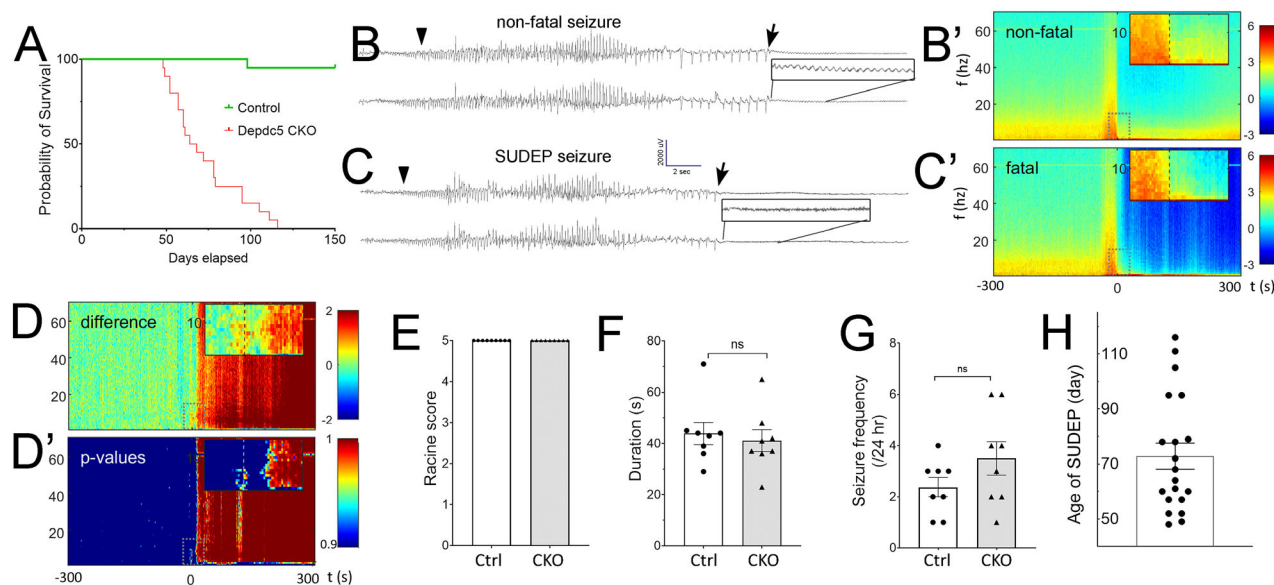


FIGURE 4: Rbp4-Cre; *Depdc5*^{F/F} CKO mice develop SUDEP. (A) Rbp4-Cre; *Depdc5*^{F/F} CKO mice (red line, $n = 20$) have a shortened lifespan and die by 4 months of age. In contrast, control (green line, $n = 19$) and *Nkx2.1-Cre; Dedpc5* CKO (data not shown) mice survive beyond 6 months. (B, C) Representative EEG examples of the last non-fatal (B) and fatal seizures (C) recorded from the same animal. The arrowhead and arrow indicate the ictal onset and ictal offset, respectively. Immediately following the ictal offset, generalized EEG suppression is seen in both non-fatal and fatal seizures. However, close-up visual examination (black boxes) reveals that low amplitude monotonous theta frequency activity is preserved only in non-fatal seizures. (B', C') Mean spectrograms showing \log^{10} (power) for non-fatal (B', $n = 16$) and fatal seizures (C', $n = 8$) in the 0–70 Hz frequency bands. Insets show –20 seconds to +30 seconds from seizure offset (time 0, dashed line) and frequencies from 0 to 15 Hz. Immediately after the ictal offset, spectrograms display decreased power in the 0 to 10 Hz band in fatal seizures, confirming the electrographic findings. (D) Difference between mean \log^{10} (power) spectrograms (non-fatal – fatal). (D') The p values that the difference between fatal and non-fatal seizures arises due to chance alone as a function of time and frequency. A significant difference ($p < 0.05$, inset) is observed immediately after the ictal offset in the theta frequency band. (E) The last non-fatal seizures and fatal seizures are generalized tonic-clonic seizures. (F) The last non-fatal and fatal seizures have similar seizure duration. (G) The seizure frequency does not increase significantly on the day of non-fatal seizures. (H) Quantification of the age of SUDEP.

of ictal apnea in the death of Rbp4-Cre; *Depdc5*^{F/F} CKO mice.

Because these animals failed to recover from ictal apnea, we next asked if they have interictal respiratory phenotypes and performed hypoxia challenge test. At baseline (normoxia), Rbp4-Cre; *Depdc5*^{F/F} CKO mice and their littermate controls had similar respiratory rates (Fig 5F, I), but Rbp4-Cre; *Depdc5*^{F/F} CKO mice showed decreased tidal volume (TV; Fig 5G, H) and minute ventilation (MV; Fig 5J, K). Upon exposure to 10% O₂ (hypoxia), Rbp4-Cre; *Depdc5*^{F/F} CKO mice and their littermate controls showed similar body temperature ($36.0 \pm 0.4^\circ\text{C}$ in control vs $36.2 \pm 0.2^\circ\text{C}$ in CKO mice, $n = 3$) and developed a similar hypoxia ventilatory response, including increased respiratory rate, TV, and MV (see Fig 5F–H, arrows). During the 20-minute challenge, control mice gradually exhibited hypoxic ventilatory depression, in which their respiratory parameters returned to baseline.²⁷ In contrast, Rbp4-Cre; *Depdc5*^{F/F} CKO mice showed a sharp and continuous decline of respiratory function (see Fig 5F–K). By the end of hypoxia challenge, their respiratory rate, TV, and MV were not only

significantly lower than control mice but also lower than their own baseline. These results suggest that Rbp4-Cre; *Depdc5*^{F/F} CKO mice have intrinsic circuit disturbances resulting in maladaptation to hypoxia.

Discussion

***Depdc5* Deletion in Cortical Layer 5 and Hippocampal Dentate Gyrus Excitatory Neurons is Sufficient to Cause Epilepsy**

The *DEPDC5* encodes the DEP domain-containing protein 5 (DEPDC5) that, together with nitrogen permease regulator 2-like (NPRL2) and nitrogen permease regulator 3-like (NPRL3), forms GATOR1 complex, the main negative regulator of the amino acids sensing machinery in the mTORC1 signaling pathway.²⁸ The mTOR pathway plays critical functions in various physiological and behavioral processes, and its aberrant hyperactivation has been linked to different pathological conditions, including epilepsy. Cell type-specific loss of the mTOR inhibition in cerebellar, dopaminergic, serotonergic, or striatal neurons induces different cognitive and behavioral deficits in the absence of epilepsy,^{29–34} suggesting that distinct cell types

and circuits are responsible for specific neuropsychiatric manifestations. Here, we showed that *Depdc5* deletion in a subset of forebrain excitatory neurons was sufficient to

cause epilepsy and SUDEP. In contrast, Nkx2.1-Cre mediated IN-specific *Depdc5* deletion did not cause spontaneous seizures, consistent with previous studies.

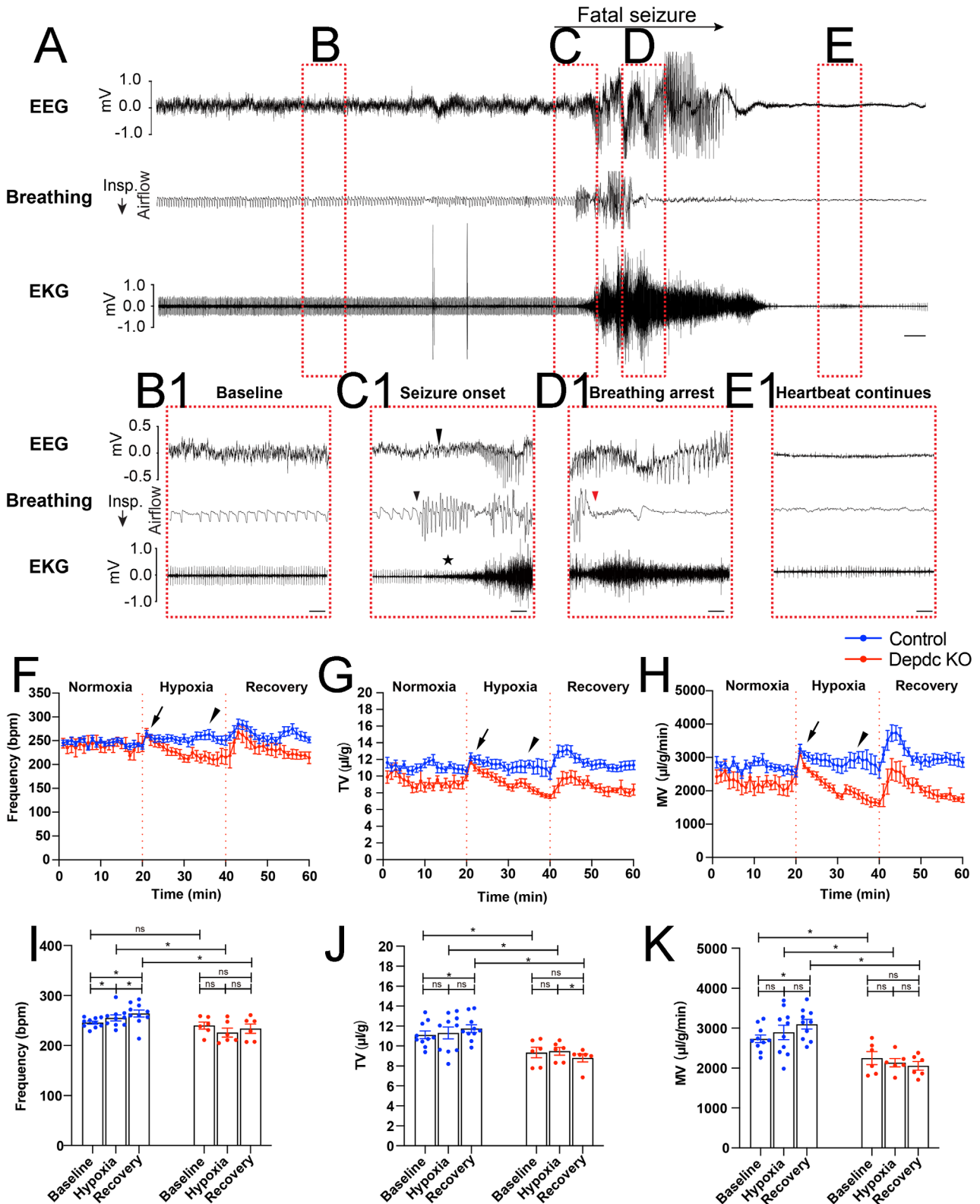


(Figure legend continues on next page.)

For example, mice with *Tsc1* deletion in PV+ or SST+ INs did not develop spontaneous seizures and grew normally into adulthood.³⁵ Mice conditionally expressing the constitutively active *Pik3ca* p.H1047R pathogenic variant in MGE-derived interneurons (Nkx2.1-Cre),³⁶ or more specifically in PV+ INs (Pvalb-Cre),³⁷ did not develop spontaneous seizures. These results suggest that mTORopathy-related epilepsy is not caused by the deletion of the mTOR pathway genes in INs. Interestingly, a recent study used a human cerebral organoid model of TSC and identified the over-proliferation of caudal late interneuron progenitor cells as a vulnerability for brain tumors and cortical malformation.³⁸ Although human-specific neurodevelopmental programs could be unique, it remains unclear whether these findings from cultured organoids representing very early embryogenesis can be translated into functional changes in more mature brains.

Although patients with familial DEPDC5-related epilepsy harbor a germline mutation, they primarily present with focal pathology in the brain.^{13,14} Genetic evidence has emerged that the focal pathology is the consequence of a pathogenic germline mutation and a somatic mutation leading to mosaic biallelic DEPDC5 loss-of-function (LOF),^{39–41} concordant with Knudson's "2-hit" hypothesis.⁴² Although our studies did not precisely recapitulate this "2-hit" genetic mechanism, Rbp4-Cre; *Depdc5*^{F/F} CKO mice modeled the mosaic biallelic LOF mutation in the brain.

Rbp4-Cre; *Depdc5*^{F/F} CKO Mice Recapitulate DEPDC5-Related Epilepsy and SUDEP

Rbp4-Cre; *Depdc5*^{F/F} CKO mice developed fatal seizures between approximately P50 and P120, equivalent to young adulthood in humans. It is noteworthy that SUDEP occurs at approximately 20 to 40 years old on

average, with a higher incidence at the younger end.⁴³ We also did a literature search and identified 8 well-documented DEPDC5-related SUDEP cases with the age of death ranging from 18 to 58 years old.^{9,11,12} Rbp4-Cre; *Depdc5*^{F/F} CKO mice developed frequent spontaneous tonic-clonic seizures, the greatest risk factor for SUDEP, and their death did not occur in the context of status epilepticus or repetitive seizures, phenocopying humans with SUDEP. These features were remarkably different from previous animal models of DEPDC5-related epilepsy. We previously generated dorsal progenitor-specific Emx1-Cre; *Depdc5*^{F/F} CKO mice that developed severe seizures and died during the third postnatal week.^{16,17} These mice developed seizure clusters, immobility, malnutrition, and wasting preceding death, making it challenging to use them for SUDEP studies. On the other hand, most Syn1-Cre; *Depdc5*^{F/F} CKO mice died of a single seizure at approximately 3 months without any prior spontaneous (clinical or subclinical) seizures, which represents an extremely rare event in patients with SUDEP.^{9,18} This is also in sharp contrast to the clinical hallmark of mTORopathies: frequent seizures. Although the strain background could slightly differ in these transgenic experiments (for example, it is unclear if previous studies used a congenic C57BL/6 Syn1-Cre strain),^{9,18} the drastic difference in seizure severity was likely caused by *Depdc5* deletion in different cell populations.

Electrographically, all fatal seizures showed immediate flattening of EEG activities upon ictal offset, which could represent post-ictal generalized EEG suppression (PGES).^{5,43} This immediate and abrupt switch from brief high amplitude ictal discharges to absolute inactivity suggests an intrinsic cerebral shutdown or an irreversible failure resulting in imminent death. PGES was proposed as a strong predictor of SUDEP, with the odds of SUDEP

FIGURE 5: Rbp4-Cre; *Depdc5*^{F/F} CKO mice develop ictal apnea and interictal respiratory dysregulation. (A) Representative EEG, breathing, and ECG traces during a spontaneous fatal seizure. Red dotted rectangles indicate (B) the baseline/pre-ictal stage, (C) the ictal onset, (D) the seizure progression, and (E) the post-ictal stage. (B1–E1) Expanded traces of (B–E). (B1) Pre-ictally, heartbeat and breathing are rhythmic. (C1) Ictal onset is marked by the arrowhead on the EEG trace. The mouse displays tachypnea with increased respiratory rate slightly before the definite electrographic onset (arrowhead on the breathing flow trace), suggesting a possible hypersynchrony involving respiratory circuits. Although the ECG trace is soon masked by muscle artifacts (*star*), there is no clear cardiac arrhythmia or irregular heartbeat at the seizure onset. (D1) Tachypnea persists in the ictal period and suddenly transitions to complete apnea (red arrowhead) in the middle of the seizure (approximately 15 seconds after the onset). (E1) During the post-ictal stage, the background suppression on EEG and the complete apnea on plethysmography continue and never recover during SUDEP. In contrast, mild bradycardia is evident on ECG and continues to worsen for several minutes leading to a terminal asystole. Scale bars: 5 seconds in A; 1 seconds in B1–E1. (F–H) Respiratory rate (bpm) (F), TV (G), and MV (H), of the Rbp4-Cre; *Depdc5*^{F/F} CKO mice (n = 6, red) and their littermate controls (n = 10, blue) before, during, and after hypoxia challenge (each period of 20 minutes). Upon exposure to a hypoxia condition, CKO mice and their littermate controls initially develop a similar hypoxia ventilatory response, including increased respiratory rate, TV, and MV (arrows). However, during the last 5 minutes of the challenge, CKO mice exhibit significantly diminished respiratory function in all 3 parameters (arrowheads). (I–K) Quantification of respiratory rate (I), tidal volume (J), and minute ventilation (K) show that *Depdc5* CKO mice (n = 6) and their littermate controls (n = 10) before, during, and after the hypoxia challenge. bpm = beats per minute; MV = minute ventilation; TV = tidal volume.

increasing by a factor of 1.7% ($p < 0.005$) with each 1-second increase in PGES duration.^{44,45} However, several follow-up studies did not reproduce these findings and showed that non-fatal generalized tonic-clonic seizures could also cause PGES. These discrepancies could be explained by heterogeneous patient populations and inherent difficulties defining PGES. PGES was defined as diffuse EEG background attenuation (eg, $< 10 \mu\text{V}$) based on the standard human 10 to 20 system scalp EEG recording^{45,46} that has relatively low sensitivity and often cannot detect low-voltage cortical activity. Therefore, non-fatal seizures could result in PGES on scalp EEG but still show clear cortical activity on intracranial EEG. The mouse EEG in our studies was obtained from screw electrodes fixed in the skull, similar to epidural electrocorticography, which could explain the high specificity of PGES in our study. Interestingly, in non-fatal seizures, the post-ictal low voltage rhythmic EEG activity and the preserved breathing rate were both in the theta frequency range. It is well-known that nasal respiration could drive neuronal oscillations.⁴⁷ Prominent respiration-entrained oscillations have been observed in the barrel cortex,⁴⁸ medial prefrontal cortex,⁴⁹ and parietal cortex,⁵⁰ during immobility, sleep, and active exploration. The post-ictal theta-frequency on EEG could represent activity driven by respiration, not the classically defined theta rhythm.

Rbp4-Cre; Depdc5^{F/F} CKO Mice Develop Ictal Apnea and Interictal Respiratory Dysfunction

In the landmark MORTEMUS study, patients who died of SUDEP in epilepsy monitoring units showed terminal apnea preceding terminal asystole.⁵¹ Several animal models also recapitulated seizure-induced respiratory arrest. For example, death could be prevented in a Dravet mouse model by mechanical ventilation and intracerebroventricular infusion of atropine, suggesting a central apnea mechanism of SUDEP.^{5,52,53} Importantly, the tonic phase-related apnea has been observed in both Dravet mice and WT mice with chemically induced seizures, suggesting a possible common SUDEP mechanism independent of epilepsy etiology.⁶ In agreement with these studies, *Rbp4-Cre; Depdc5^{F/F}* CKO mice developed ictal apnea before cardiac asystole during fatal seizures and, more interestingly, had baseline respiratory dysregulation.

It remains unclear how seizures lead to respiratory arrest in SUDEP, but there are several possibilities. First, direct and indirect projections from the cortex to brainstem respiratory centers could be the anatomic substrate for seizure-induced respiratory dysfunction. Generalized seizures drive dual inhibition on the central respiratory and cardiac pathways resulting in ictal apnea and bradycardia.⁵⁴ In addition, it is possible that seizures

alter cellular or neural network function, leading to progressive respiratory disruption and increased SUDEP propensity. Radiographic and pathological studies indeed showed structural and cytoarchitectural abnormalities in the ventral lateral and raphe regions of the medulla, which both play important roles in central respiratory regulation.⁵⁵ Recurrent seizures could trigger extensive gliosis in those areas resulting in respiratory abnormalities and premature mortality.⁵⁶ Concordantly, the inadequate response to hypoxia in *Rbp4-Cre; Depdc5^{F/F}* CKO mice suggests that the breathing circuit develops increased vulnerability to severe seizures over time that results in respiratory decompensation and, ultimately, failure. A second possibility is that defective molecular programs in respiratory control regions make the breathing circuit more vulnerable to seizures. For example, neurons in breathing control regions express ion channels important for respiratory functions. In a Dravet syndrome mouse model, expression of an SCN1A pathogenic variant in inhibitory neurons in the retrotrapezoid nucleus, a key brainstem region in the breathing circuit, resulted in defective chemosensation and SUDEP.⁵⁷ A third possibility is that developmentally accumulated molecular and cellular defects induced by recurrent seizures, together with intrinsically perturbed homeostasis due to gene mutations, progressively increase the susceptibility of critical respiratory centers to failure during generalized tonic-clonic seizures.

In summary, our study provides a novel animal model of DEPDC5-related epilepsy and SUDEP with good construct and face validity, paving the way to parse out the pathophysiology at molecular, cellular, and circuit levels.

Acknowledgments

The authors thank Dr Kenneth Kwan for donating the *Rbp4-Cre* transgenic mice. We also thank Dr Jun Hee Lee for donating the floxed *Depdc5* conditional knockout mice.

Author Contributions

Y.W. and P.L. contributed to the conception and design of the study. H.Y.K., Y.Y., T.Y., J.Z., M.Z., M.Y.M., S.H., R.C., S.W., N.N.B., and R.B. contributed to the acquisition and analysis of data. Y.W., P.L., D.K.L., J.M.P., H.K.Y., Y.Y., and T.Y. contributed to drafting the text or preparing the figures.

Potential Conflicts of Interest

All authors declared no potential conflicts of interest.

Data Availability

Raw data, materials, and reagents of this study are available from the corresponding authors (Y.W. and P.L.) on request.

References

- Harden C, Tomson T, Gloss D, et al. Practice guideline summary: sudden unexpected death in epilepsy incidence rates and risk factors: report of the guideline development, dissemination, and implementation Subcommittee of the American Academy of Neurology and the American Epilepsy Society. *Neurology* 2017;88:1674–1680.
- Li R, Buchanan GF. Scrambling to understand sudden unexpected death in epilepsy: insights from animal models. *Epilepsy Curr* 2019;19:390–396.
- Kearney J. Sudden unexpected death in dravet syndrome. *Epilepsy Curr* 2013;13:264–265.
- Costagliola G, Orsini A, Coll M, et al. The brain-heart interaction in epilepsy: implications for diagnosis, therapy, and SUDEP prevention. *Ann Clin Transl Neurol* 2021;8:1557–1568.
- Kim Y, Bravo E, Thimbeck CK, et al. Severe peri-ictal respiratory dysfunction is common in Dravet syndrome. *J Clin Invest* 2018;128:1141–1153.
- Wenker IC, Teran FA, Wengert ER, et al. Postictal death is associated with tonic phase apnea in a mouse model of sudden unexpected death in epilepsy. *Ann Neurol* 2021;89:1023–1035.
- Dibbens LM, de Vries B, Donatello S, et al. Mutations in DEPDC5 cause familial focal epilepsy with variable foci. *Nat Genet* 2013;45:546–551.
- Epi4K consortium, Epilepsy Phenome/Genome P. Ultra-rare genetic variation in common epilepsies: a case-control sequencing study. *Lancet Neurol* 2017;16:135–143.
- Bacq A, Roussel D, Bonduelle T, et al. Cardiac investigations in sudden unexpected death in DEPDC5-related epilepsy. *Ann Neurol* 2022;91:101–116.
- Bagnall RD, Crompton DE, Petrovski S, et al. Exome-based analysis of cardiac arrhythmia, respiratory control, and epilepsy genes in sudden unexpected death in epilepsy. *Ann Neurol* 2016;79:522–534.
- Weckhuysen S, Marsan E, Lambrecq V, et al. Involvement of GATOR complex genes in familial focal epilepsies and focal cortical dysplasia. *Epilepsia* 2016;57:994–1003.
- Nascimento FA, Borlot F, Cossette P, et al. Two definite cases of sudden unexpected death in epilepsy in a family with a DEPDC5 mutation. *Neurol Genet* 2015;1:e28.
- Baldassari S, Picard F, Verbeek NE, et al. The landscape of epilepsy-related GATOR1 variants. *Genet Med* 2019;21:398–408.
- Figlia G, Muller S, Hagenston AM, et al. Brain-enriched RagB isoforms regulate the dynamics of mTORC1 activity through GATOR1 inhibition. *Nat Cell Biol* 2022;24:1407–1421.
- Holmes GL, Stafstrom CE, Tuberous Sclerosis Study G. Tuberous sclerosis complex and epilepsy: recent developments and future challenges. *Epilepsia* 2007;48:617–630.
- Yang T, Hu S, Chang WC, et al. Perineuronal nets degradation and parvalbumin interneuron loss in a mouse model of DEPDC5-related epilepsy. *Dev Neurosci* 2022;44:671–677.
- Klofas LK, Short BP, Zhou C, Carson RP. Prevention of premature death and seizures in a Depdc5 mouse epilepsy model through inhibition of mTORC1. *Hum Mol Genet* 2020;29:1365–1377.
- Yuskaitis CJ, Jones BM, Wolfson RL, et al. A mouse model of DEPDC5-related epilepsy: neuronal loss of Depdc5 causes dysplastic and ectopic neurons, increased mTOR signaling, and seizure susceptibility. *Neurobiol Dis* 2018;111:91–101.
- Hu S, Knowlton RC, Watson BO, et al. Somatic Depdc5 deletion recapitulates electroclinical features of human focal cortical dysplasia type IIA. *Ann Neurol* 2018;84:140–146.
- Drorbaugh JE, Fenn WO. A barometric method for measuring ventilation in newborn infants. *Pediatrics* 1955;16:81–87.
- Leone DP, Heavner WE, Ferenczi EA, et al. Satb2 regulates the differentiation of both callosal and subcerebral projection neurons in the developing cerebral cortex. *Cereb Cortex* 2015;25:3406–3419.
- Madisen L, Zwingman TA, Sunkin SM, et al. A robust and high-throughput Cre reporting and characterization system for the whole mouse brain. *Nat Neurosci* 2010;13:133–140.
- Racine RJ. Modification of seizure activity by electrical stimulation. II. Motor seizure. *Electroencephalogr Clin Neurophysiol* 1972;32:281–294.
- Xu Q, Tam M, Anderson SA. Fate mapping Nkx2.1-lineage cells in the mouse telencephalon. *J Comp Neurol* 2008;506:16–29.
- Wonders CP, Taylor L, Welagen J, et al. A spatial bias for the origins of interneuron subgroups within the medial ganglionic eminence. *Dev Biol* 2008;314:127–136.
- Tremblay R, Lee S, Rudy B. GABAergic interneurons in the neocortex: from cellular properties to circuits. *Neuron* 2016;91:260–292.
- Yao Y, Chen J, Li X, et al. A carotid body-brainstem neural circuit mediates sighing in hypoxia. *Curr Biol* 2023;33:827–37 e4.
- Bar-Peled L, Chantranupong L, Cherniack AD, et al. A tumor suppressor complex with GAP activity for the rag GTPases that signal amino acid sufficiency to mTORC1. *Science* 2013;340:1100–1106.
- Clipperton-Allen AE, Page DT. Pten haploinsufficient mice show broad brain overgrowth but selective impairments in autism-relevant behavioral tests. *Hum Mol Genet* 2014;23:3490–3505.
- Tsai PT, Hull C, Chu Y, et al. Autistic-like behaviour and cerebellar dysfunction in Purkinje cell Tsc1 mutant mice. *Nature* 2012;488:647–651.
- Kosillo P, Doig NM, Ahmed KM, et al. Tsc1-mTORC1 signaling controls striatal dopamine release and cognitive flexibility. *Nat Commun* 2019;10:5426.
- McMahon JJ, Yu W, Yang J, et al. Seizure-dependent mTOR activation in 5-HT neurons promotes autism-like behaviors in mice. *Neurobiol Dis* 2015;73:296–306.
- Benthall KN, Cording KR, Agopyan-Miu A, et al. Loss of Tsc1 from striatal direct pathway neurons impairs endocannabinoid-LTD and enhances motor routine learning. *Cell Rep* 2022;38:110563.
- Normand EA, Crandall SR, Thorn CA, et al. Temporal and mosaic Tsc1 deletion in the developing thalamus disrupts thalamocortical circuitry, neural function, and behavior. *Neuron* 2013;78:895–909.
- Zhao JP, Yoshii A. Hyperexcitability of the local cortical circuit in mouse models of tuberous sclerosis complex. *Mol Brain* 2019;12:6.
- D’Gama AM, Woodworth MB, Hossain AA, et al. Somatic mutations activating the mTOR pathway in dorsal telencephalic progenitors cause a continuum of cortical Dysplasias. *Cell Rep* 2017;21:3754–3766.
- Sharma V, Sood R, Lou D, et al. 4E-BP2-dependent translation in parvalbumin neurons controls epileptic seizure threshold. *Proc Natl Acad Sci U S A* 2021;118:e2025522118.
- Eichmuller OL, Corsini NS, Vertesy A, et al. Amplification of human interneuron progenitors promotes brain tumors and neurological defects. *Science* 2022;375:eabf5546.
- Baldassari S, Ribierre T, Marsan E, et al. Dissecting the genetic basis of focal cortical dysplasia: a large cohort study. *Acta Neuropathol* 2019;138:885–900.
- Lee WS, Stephenson SEM, Howell KB, et al. Second-hit DEPDC5 mutation is limited to dysmorphic neurons in cortical dysplasia type IIA. *Ann Clin Transl Neurol* 2019;6:1338–1344.

41. Ribierre T, Deleuze C, Bacq A, et al. Second-hit mosaic mutation in mTORC1 repressor DEPDC5 causes focal cortical dysplasia-associated epilepsy. *J Clin Invest* 2018;128:2452–2458.
42. Knudson AG. Two genetic hits (more or less) to cancer. *Nat Rev Cancer* 2001;1:157–162.
43. Tomson T, Walczak T, Sillanpaa M, Sander JW. Sudden unexpected death in epilepsy: a review of incidence and risk factors. *Epilepsia* 2005;46:54–61.
44. Carlson C. Generalized postictal EEG background suppression: a marker of SUDEP risk. *Epilepsy Curr* 2011;11:86–87.
45. Lhatoo SD, Faulkner HJ, Dembny K, et al. An electroclinical case-control study of sudden unexpected death in epilepsy. *Ann Neurol* 2010;68:787–796.
46. Tao JX, Yung I, Lee A, et al. Tonic phase of a generalized convulsive seizure is an independent predictor of postictal generalized EEG suppression. *Epilepsia* 2013;54:858–865.
47. Tort ABL, Brankack J, Draguhn A. Respiration-entrained brain rhythms are global but often overlooked. *Trends Neurosci* 2018;41:186–197.
48. Ito J, Roy S, Liu Y, et al. Whisker barrel cortex delta oscillations and gamma power in the awake mouse are linked to respiration. *Nat Commun* 2014;5:3572.
49. Biskamp J, Bartos M, Sauer JF. Organization of prefrontal network activity by respiration-related oscillations. *Sci Rep* 2017;7:45508.
50. Tort ABL, Ponsel S, Jessberger J, et al. Parallel detection of theta and respiration-coupled oscillations throughout the mouse brain. *Sci Rep* 2018;8:6432.
51. Ryvlin P, Nashef L, Tomson T. Prevention of sudden unexpected death in epilepsy: a realistic goal? *Epilepsia* 2013;54:23–28.
52. Massey CA, Sowers LP, Dlouhy BJ, Richerson GB. Mechanisms of sudden unexpected death in epilepsy: the pathway to prevention. *Nat Rev Neurol* 2014;10:271–282.
53. Goldman AM. When apnea turns terminal: when, how, why? *Epilepsy Curr* 2021;21:449–451.
54. Schilling WP, McGrath MK, Yang T, et al. Simultaneous cardiac and respiratory inhibition during seizure precedes death in the DBA/1 audiogenic mouse model of SUDEP. *PLoS One* 2019;14:e0223468.
55. Patodia S, Tachrount M, Somani A, et al. MRI and pathology correlations in the medulla in sudden unexpected death in epilepsy (SUDEP): a postmortem study. *Neuropathol Appl Neurobiol* 2021;47:157–170.
56. Dhaibar HA, Hamilton KA, Glasscock E. Kv1.1 subunits localize to cardiorespiratory brain networks in mice where their absence induces astrogliosis and microgliosis. *Mol Cell Neurosci* 2021;113:103615.
57. Kuo FS, Cleary CM, LoTurco JJ, et al. Disordered breathing in a mouse model of Dravet syndrome. *Elife* 2019;8:e43387.